Compliance Engineering®

Antenna Pattern Measurement: Concepts and Techniques

Michael D. Foegelle

As high frequencies become more common, understanding antenna pattern measurement and how to obtain useful measurements becomes critical.

The first article of this two-part series explores the basic concepts and techniques of antenna pattern measurement and evaluates the benefits and drawbacks of various measurement methods. The concepts relating to near-field and far-field pattern testing are discussed as well. The second article (see page 34) presents the theory and equations governing antenna properties and includes a complete description of a site calibration for pattern-measurement testing.

Antenna pattern measurement refers to the determination of the radiation pattern of an antenna under test (AUT). It is the measurement of the relative magnitude and phase of an electromagnetic signal received from the AUT. Although highly directional antennas (i.e., horns) are often measured by scanning a plane perpendicular to the bore-sight axis of the antenna (i.e., parallel to the face of the horn) at some distance, this article focuses on total spherical pattern measurements. A subset of this is the simple polar planar cut, in which the pattern is determined for a single azimuth rotation around the antenna.

Because a passive antenna is reciprocal, the pattern information could be obtained by using it as either the transmitter or receiver. This is in contrast to an active antenna system, in which transmit and receive behavior may be considerably different, and thus both relative pattern and absolute power information is required. In addition to the relative information that makes up the antenna pattern itself, and the various pieces of information that can be determined from it, a variety of other results can be determined from an active antenna system.

Although complex antenna-pattern measurement has been a common requirement in the microwave antenna arena for many years, it has only recently become more common to other areas such as electromagnetic compatibility (EMC) and wireless telecommunication. On the EMC front, the interest in pattern measurements appears to stem from a range of sources. The first is that, as EMC standards are forced to move higher in frequency, the effects of narrow-beam radiation from the equipment under test (EUT) and the corresponding interaction with the receive antenna become increasingly significant. It is important that the test antenna is able to see all signals radiating from the EUT. In addition, broadband antennas designed for EMC work are finding their way into other applications in which concern for antenna patterns has always been an issue. Finally, many engineers with microwave backgrounds now must deal with EMC issues. These engineers want more information than has traditionally been provided on these antennas.

For the wireless industry, base station antenna patterns have always been important in ensuring coverage. Understanding the pattern of each cell tower is critical to determining the required spacing between them. However, lately the industry has put considerable

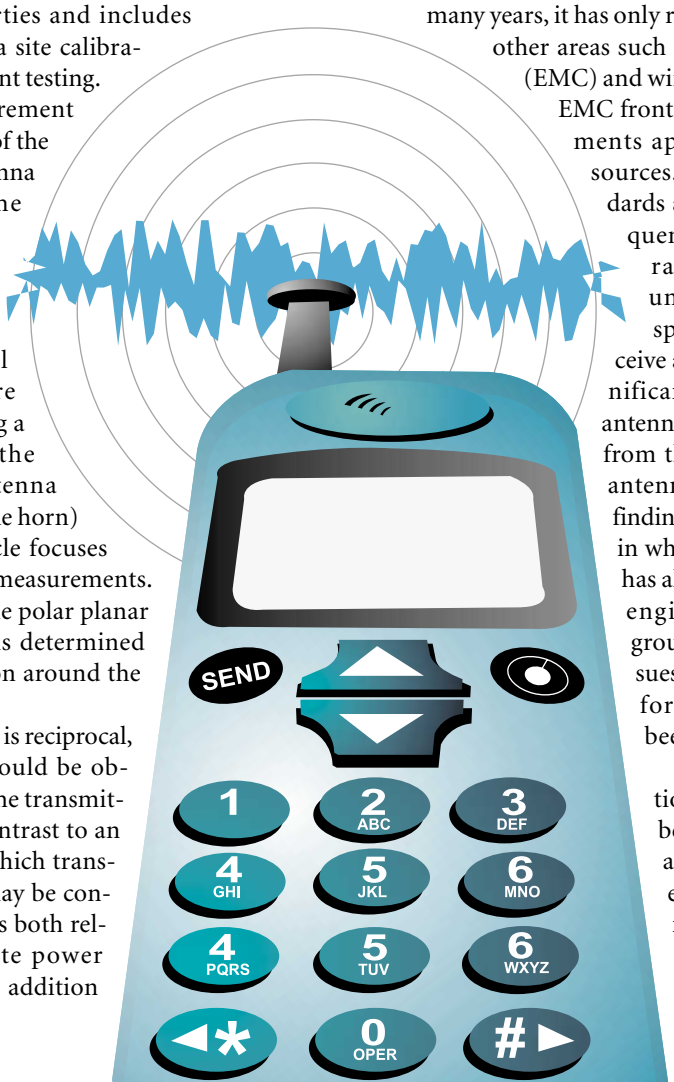

Illustration by TAISHA PAYTON

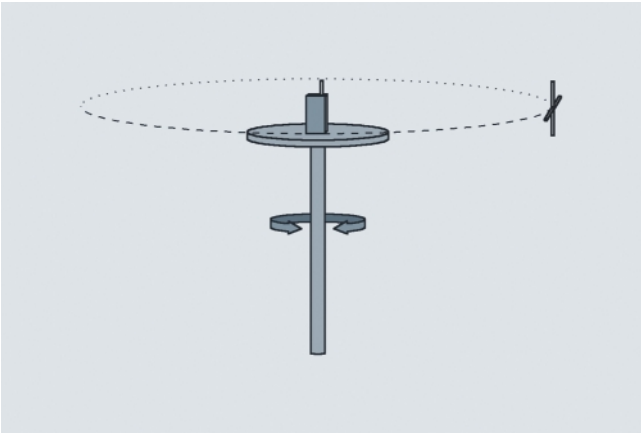

Figure 1. Test setup for single-axis polar pattern measurement.

emphasis on handset pattern measurement as well.

The Cellular Telecommunications and Internet Association (CTIA) has drafted a set of test plans aimed at verifying the performance of cellular telephone handsets. One of the CTIA plans provides tests for verifying radiated signal performance.[1]

Previously, cell phones were required to meet a peak-signal requirement, but now they are required to meet a total radiated power requirement. This requirement ensures that a cell phone is transmitting energy in a broad pattern rather than in a narrow beam and, therefore, is less likely to lose contact with the cellular network.

The tests are also designed to characterize both transmitted and received power and pattern, as well as the minimum signal that the phone can properly detect. There are also calculations designed to determine the effectiveness of the phone when the base station antennas are located along the horizon (the typical configuration). The tests help to ensure that not all of the radiated energy is directed up into space or down into the ground.

Whereas cell phone manufacturers are often interested in the performance of the phone by itself, CTIA also requires testing with a liquid-filled phantom head or torso to simulate the effect of human interaction with the phone.

In addition to cell phones, other products with growing wireless testing requirements include wireless personal digital assistants, which are typically covered under the cellular requirements, and home- and office-based wireless networks such as wireless local-area networks and Bluetooth devices.

Measurement Techniques

The basic pattern-measurement technique that most people are familiar with uses a single-axis rotational pattern. This technique involves an AUT placed on a rotational positioner and rotated about the azimuth to generate a two-dimensional polar pattern. This measurement is commonly done for the two principal axes of the antenna to determine parameters such as antenna beam width in both the E and H planes. Such data are typically only measured for the copolar field component for simple horns or dipoles for which the general polarization of the pattern is well known.

For more-complicated radiators, for which the polarization may not be known, or may vary as a function of angle, it is important to be able to measure two orthonormal (i.e., perpendicular) field components. This measurement is usually accomplished by using a dual-polarized horn, log-periodic dipole array, or dipole antenna as the measurement antenna (MA). Although it provides the best result, this technique requires two receivers or the ability to automatically switch the polarization of a single receiver, which can increase the cost of the test. A slower, and possibly less accurate, option is to repeat an identical pattern test for each MA polarization. This option could result in time variations and alignment issues that could have significant effects.

Figure 1 shows a typical polar-pattern test setup. The AUT (a cell phone in this case) is placed on a rotating turntable, and a dual-polarized antenna is placed level with the AUT a fixed distance away. The turntable is rotated 360°, and the response between the antennas is measured as a function of angle. Normally, these measurements are performed in a fully anechoic (simulated free-space) environment, but sometimes it may be desirable to measure the pattern over conducting ground, or in some other as-used geometry to get real-world pattern information. Figure 2 shows some polar patterns for typical antenna types and polarizations.

To generate a full spherical-pattern measurement, it is necessary to change the relationship between the AUT and the MA and repeat the previous polar test for each new orientation. The changes in orientation must be perpendicular to the plane of measurement to completely cover a spherical surface. In simpler terms, the second axis of rotation must be perpendicular to and intersect the first axis of rotation.

The two axes correspond to the θ and ϕ angles of the spherical coordinate system and are typically referred to as *elevation* and *azimuth*, respectively. Just as in the spherical coordinate system, only one axis needs to be rotated through 360°, whereas the other is rotated only through 180°. With the proper processing of the resulting data, it really does not matter which axis is which. Either antenna can be rotated around this second axis to generate the same pattern, but each technique has both advantages and disadvantages.

Conical-Section Method

The conical-section method uses an elevated turntable to support the AUT and rotates the MA around the AUT on an axis perpendicular to the vertical rotational axis of the turntable (see Figure 3). This method fits the geometric picture that most people have for spherical coordinate systems, and, therefore, it is often the method used for pattern measurements. The turntable continues to provide the azimuth (ϕ) rotation, whereas the MA is raised (elevated) or lowered in an arc around the AUT, and, thus, the term *elevation axis*.

A common misconception when visualizing this technique is to consider moving the MA in a 180° arc across the top of the AUT. However, a quick look at Figure 3 shows that this would just duplicate the measurement across the top half of the AUT and never measure the bottom half of the pattern. The data points at ($\phi = 0°$, $\theta = +x°$) and ($\phi = 180°$, $\theta = -x°$), where $\theta = 0°$ directly above the antenna, are the same.

This method results in the MA describing circles of varying diameter, and thus the reference to conical sections. The circles may be thought of as latitude lines on a globe, from the north ($+z$) to south ($-z$) poles, with the largest circle located

at the equator. Only the one circle where the MA is at the same height as the AUT (i.e., the equator) results in a true polar pattern measurement.

Although the conical-section method is conceptually simple, it has a number of drawbacks. A large pivot arm or arch support is required to manipulate the MA. For long range lengths, this requirement can be a difficult proposition. Similarly, if this test is to be performed in a fully anechoic chamber, the chamber must be much larger than would normally be necessary to support the required range length because the floor and ceiling must be the same distance away as the rear wall behind the MA. This can dramatically increase the cost of antenna measurement.

To perform a full surface measurement, the turntable must also be cantilevered out from a wall or other support to allow the MA to be moved under the turntable. Otherwise, there will be a dead zone where the antenna is blocked by the supporting structure. In any case, the turntable itself can significantly affect the pattern measured if it is too massive or made of the wrong materials.

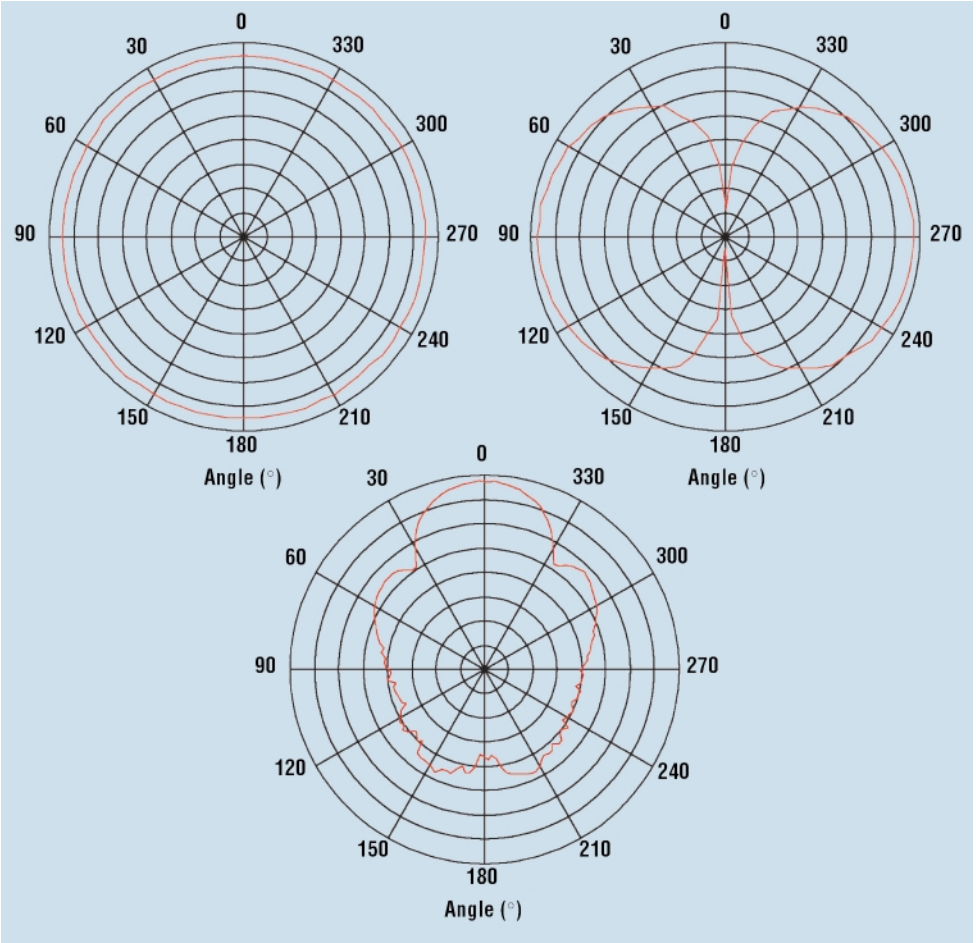

Figure 2. Copolarized polar patterns for a vertically polarized dipole, horizontally polarized dipole, and standard-gain horn.

Great-Circle Method

For the great-circle method, the MA is fixed and the AUT is repositioned on the turntable to generate each polar cut. Because the MA is fixed, pointing perpendicular to the rotation axis in this case, every cut is a true polar pattern. Therefore, each rotation of the turntable provides the greatest diameter circle possible.

To compare the two methods, the AUT must be laid on its side with respect to the setup for the conical-section method to represent the associated shift in coordinate systems (see Figure 4).

By rotating the AUT about the horizontal axis between each great-circle cut, the entire spherical surface can be covered (see Figure 5). Each polar cut passes through the others at the horizontal axis of rotation, and the intersection points at the horizontal axis are equivalent to the top and bottom MA positions in the conical-section method. This is why the AUT was laid on its side, to support the change in coordinates.

For the great-circle method, the circles can be thought of as longitude lines, running from the north ($+z$) to the south ($-z$) pole and back around the other side. As before, it is only necessary to rotate the AUT (instead of the MA) through 180° to cover the entire sphere because the great circles cover the front and back of the sphere simultaneously.

With the shift in coordinate systems, the turntable is now an elevation positioner rather than an azimuth positioner because it changes the MA position from pole to pole rather than along latitudinal lines parallel to the equator. The horizontal rotation axis of the AUT now provides the azimuth positioning.

The great-circle method has the advantage of being relatively easy to perform with a low-cost system by rotating the AUT manually about the horizontal axis, but, as with most such endeavors, it can be extremely tedious without additional automation. The method has an added benefit. The path between the AUT and MA is never obscured by the support structure, although care must be taken to ensure that the existing support structure does not have reflective properties that could alter the antenna pattern, especially if additional material is required to support the AUT in different orientations.

Finally, because the MA is fixed, the chamber only needs to support the required range length in one dimension. This opens the possibility of using tapered chambers and the like to obtain high performance and long range lengths affordably.

Comparison of Methods

Although each method has advantages and disadvantages, it is important to verify that they are both capable of produc-

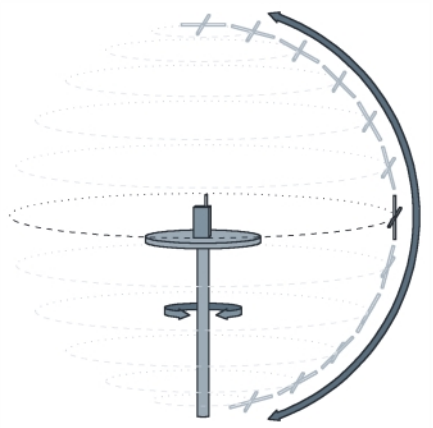

Figure 3. Illustration of the conical-section method for spherical antenna-pattern measurement.

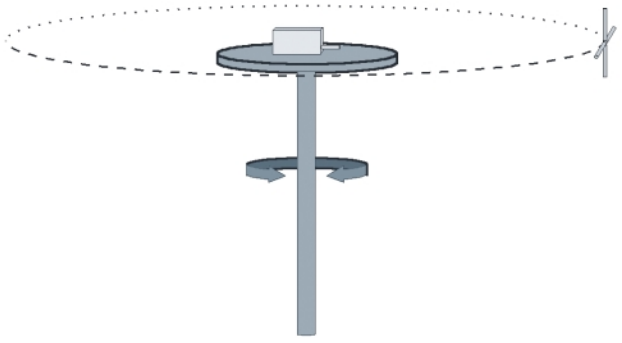

Figure 4. Great-circle configuration of antenna under test.

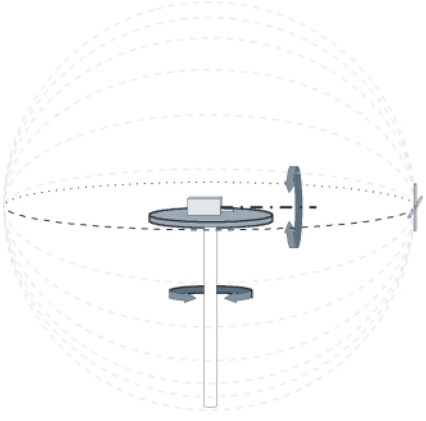

Figure 5. Illustration of the great-circle method for spherical antenna-pattern measurement. The back sides of the polar cuts have been removed for clarity.

ing the same results. Figure 6 shows both conical section (a) and great circle (b) results with the same step size between measurement points and in which the coordinate systems have been aligned. Overlaying the two plots (see Figure 6c) shows that the actual measured data points are identical, regardless of the method used. Therefore, given just the resulting data points (see Figure 6d), it is not possible to determine which method was used to generate them.

Two-Axis Positioners

By adopting the great-circle method and manipulating the AUT in two axes, it is possible to automate the test such that data can be acquired according to the measurement sequence of either method. Figure 7 shows a simple two-axis positioner that can automate the rotation of the AUT on both axes. By rotating the turntable (elevation) 360° and stepping the horizontal axis (azimuth) of the AUT between each turntable rotation, the great-circle method (see Figure 8a) can be duplicated. Alternatively, by rotating the horizontal axis (azimuth) of the AUT 360° and stepping the turntable (elevation), the conical-section method (see Figure 8b) can be duplicated.

The two-axis positioner does suffer from one of the limitations mentioned for the conical-section method. That is, for some portion of the pattern (the south pole in Figures 7 and 8), the support structure is between the AUT and the MA. This effect can be minimized by matching the support structure to the load being rotated, thereby reducing the amount of interposing material to a minimum. Controlling the orientation of the AUT with respect to the support can also improve results. By making sure that the support is in a null or back-lobe, its effects on pattern-related measurements can be minimized.

Three-Dimensional Patterns

No matter which method is used to acquire the data, the analysis of the result is made easier by the use of a three-dimensional spherical plot to graph the output. Figure 9 gives an example of a dipole pattern (a) and a standard-gain horn pattern (b) plotted in three dimensions. This type of graphing capability allows the pattern to be rotated around for different views to help get an idea of the relative magnitude of the signal in various directions.

Near-Field versus Far-Field Measurements

Regardless of how the data are acquired, one of the available system variables is the range length. Usually, when one refers to the properties of an antenna, be it antenna pattern, gain, or another property, the reference is to the far-field, free-space properties of the antenna. In the far-field, free-space condition, the measured properties of the antenna do not appear to vary as a function of separation distance or antenna location. That is not to say that the measured field levels themselves do not vary, but that the measured gain or pattern does not vary. To state it simply, the far-field, free-space condition is the condition in which all of the theoretical equations typically used for calculating antenna properties are valid.

In a near-field or non-free-space environment, the antenna properties that are measured appear to vary as a function of their environment. Effects such as mutual coupling between the AUT and the measurement antenna or the antennas and other objects around them, as well as other near-field perturbations, prevent the direct determination of the desired antenna properties. Even assuming a good free-space environment (i.e., a fully anechoic chamber), there are still limitations to near-field testing.

Most readers will be familiar with at least one rule of thumb for near- versus far-field determinations. In reality, there are two very different definitions. The first, which is usually more

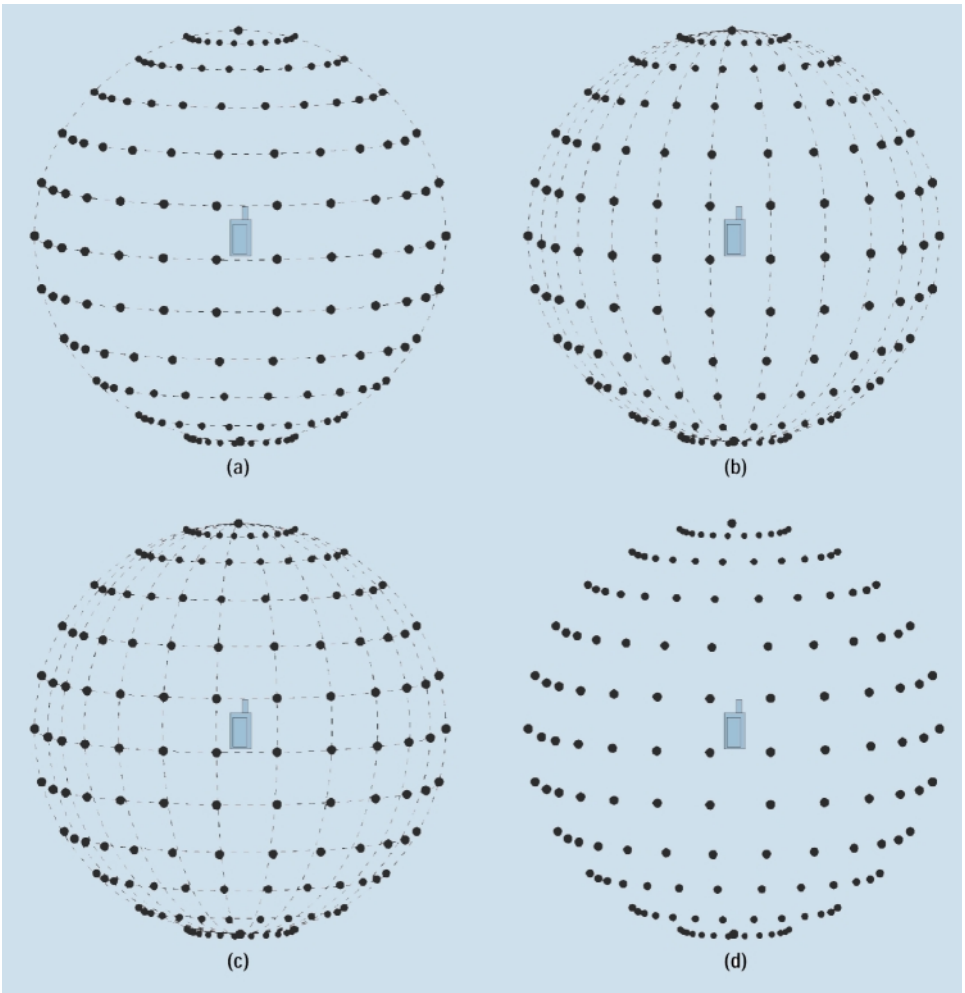

Figure 6. Comparison of measurement points between (6a) conical-section method and (6b) great-circle method. (6c) shows the two results overlaid, and (6d) indicates that it is impossible to tell which method was used given only the resulting data points.

The second far-field requirement, which is more famil- iar to microwave engineers, is usually the dominant factor at higher frequencies. In this case, the objects involved (either the actual antennas or larger devices containing small antennas) are large compared with the wavelength.

The effects of scattering from different points on the object, or from different emissions points in the case of an antenna array or a leaky shielded enclosure with multiple openings, result in wave fronts propagating in multiple directions. The far-field condition is met when all of these different wave fronts merge to form one wave front; that is, when the multiple sources are indistinguishable from a single source (when separation distance $r > 2D^2/\lambda$).

Therefore, the bigger the object or the shorter the wavelength, the farther away the receive antenna has to be for that object to appear as a single source. The region inside the $2D^2/\lambda$ distance, but outside the reactive near-field region, is referred to as the *radiating near-field* or *Fresnel region*, whereas the region outside this distance is the *far-field* or *Fraunhofer region*.[2]

important at low frequencies, is represented by the near-field term(s) of the electric and/or magnetic field equations. These are the terms that behave as $1/r^n$, where $n > 1$. These terms represent the nonpropagating or evanescent electric and magnetic fields—those caused by capacitively or inductively stored energy in the antenna. Therefore, this region is referred to as the reactive region of the antenna.[2]

The reactive fields decay rapidly with distance from the antenna, leaving only the $\vec{E} \times \vec{H}$ term, which has a $1/r$ behavior. In this case, the far-field condition is satisfied by $\lambda/r << 1$, that is, where the measurement distance r is much greater than wavelength λ. The reactive region is commonly defined as

$$r < 0.62 \sqrt{D^3/\lambda} \ ,$$

where D is the largest dimension of the radiating object. For practical applications, a simple rule of thumb suitable for most antennas is given by $r < 2\lambda$. Within this region, any measurement antenna or probe would have a significant effect on the transmit antenna.

In terms of antenna-pattern measurements, normally there is little useful information to be gained within the reactive region of an antenna. The one possible exception would be when the antenna is to be used in the reactive region as well.

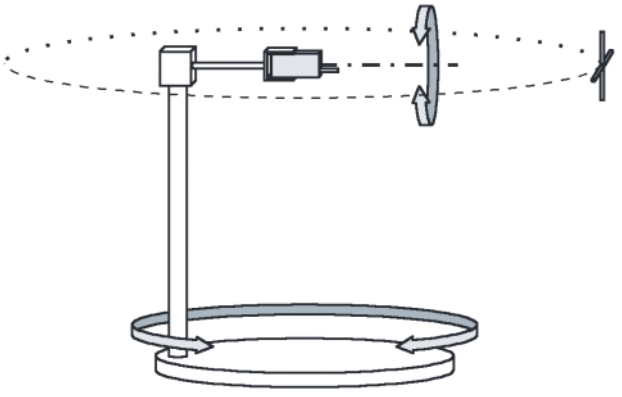

Figure 7. Example of a two-axis positioner setup for pattern-measurement testing.

However, it would not be possible to eliminate the effect of the measurement antenna on the AUT, and therefore the usefulness of such data would be limited. The Fresnel region contains propagating electromagnetic energy, but not in a cohesive form. Therefore, pattern measurements done in this region can readily determine quantities such as total radiated power but may only provide an approximation of the far-field pattern, gain, and other properties.

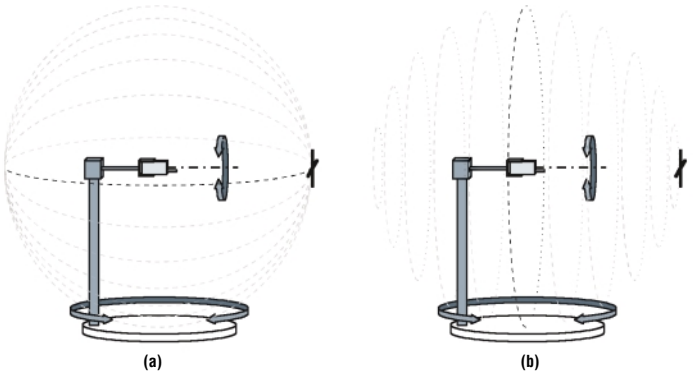

Figure 8. (a) Great-circle method and (b) conical-section method performed using the same two-axis positioner.

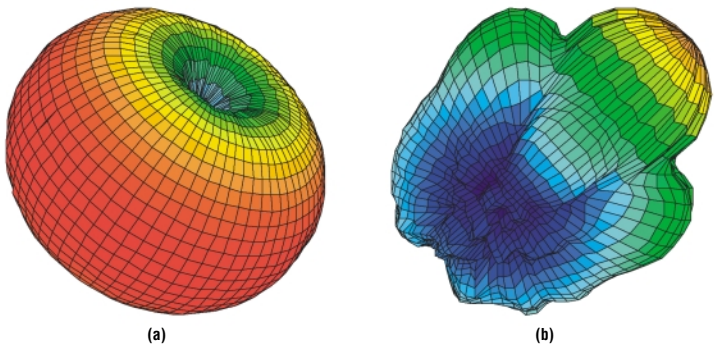

Figure 9. Three-dimensional spherical plot of (a) simple dipole and (b) standard-gain horn. Note the expected toroidal (donut) shape of the dipole pattern and the strong directionality and sidelobes of the standard-gain horn.

Converting from Near Field to Far Field

A common practice in microwave antenna measurements, and something of a Holy Grail for EMC measurements, is the use of near-field measurements to predict far-field results. In the Fresnel region, it is possible to scan the magnitude and phase of the field along a closed surface (or, in the case of planar near-field scanning, an open surface intersecting the vast majority of the propagating energy) and predict the far-field levels. Acquiring the relative phase and magnitude at each point on the surface requires the use of a reference signal in addition to the measurement antenna signal. The fixed reference is needed to track the relative phase of the signal in time because each point in space is not sampled at the same instant in time.

For passive antennas, a vector network analyzer is normally used, which acquires both magnitude and phase information against its own reference signal. Active devices are more complicated, requiring the use of a fixed reference antenna or sensor in addition to the measurement antenna to obtain both phase and magnitude references (because an active device may not maintain a constant magnitude or phase relationship). In either case, the calculations required to do the conversion are beyond the scope of this article.

For EMC testing, the conversion of radiated-emissions measurements from near field to far field is made much more difficult by the nature of the electromagnetic signature of the device under test and the frequency range required for EMC testing. EMC emissions are far from being continuous wave, often consisting of harmonics, broadband noise, and spurious signals. Obtaining the same radiation signature at each point of a near-field scan is very unlikely.

To further complicate matters, low-frequency EMC measurements are often performed in the reactive region of both the EUT and the receive antenna. Although near-field reactive terms can be easily determined for simple dipole elements, such predictions for more-complicated antennas or emitters are extremely difficult. The amount of data and processing required to correctly separate the effects of the EUT from the receive antenna and the rest of the environment to truly predict a far-field result is far beyond the current state of the art.

Conclusion

The need for antenna-pattern information is increasing as the EMC community moves to higher frequencies and more-advanced techniques, and as wireless devices continue to pervade our everyday radio-frequency (RF) environment. The techniques for complex-pattern measurement are rather straightforward, but there are some pitfalls. Useful pattern information can be obtained using either the radiating near-field or far-field, but not the reactive, region of the AUT. The conversion of near-field pattern information to far-field results is possible, but it requires specialized software and measurement capabilities.

References

1. "Method of Measurement for Radiated RF Power and Receiver Performance, Draft Revision 1.2" (Washington, DC: CTIA, 2001).
2. CA Balanis, *Antenna Theory, Analysis and Design* (New York: Harper & Row, 1982), 22–23.

Michael D. Foegelle, PhD, is senior principal design engineer at ETS-Lindgren (Cedar Park, TX). He can be reached at 512-531-6444 or michael.foegelle@emctest.com. ■

Antenna Pattern Measurement: Theory and Equations

Michael D. Foegelle

The second installment on antenna pattern measurement describes the calculations involved in determining properties such as TRP, EIRP, directivity, and efficiency.

This is the second article in a two-part series on antenna pattern measurement. This installment presents the theory and equations governing a variety of antenna properties and includes a complete description of a site calibration for pattern-measurement testing.

Illustration by TAISHA PAYTON

Range Calibration

With a two-axis positioner setup, it is quite straightforward to perform general pattern measurements and determine a variety of relative data such as 3-dB beam width, front-to-back ratio, and directivity. However, before accurate measurements of values such as total radiated power (TRP), effective isotropic radiated power (EIRP), or antenna gain can be made, it is necessary to perform a reference calibration to correct for the various factors affecting these tests. The factors include components such as range-length loss, gain of the receive antenna, cable losses, and so forth.

Normally, this calibration is done using a reference antenna (typically either a dipole or standard-gain horn) with known gain characteristics. The reference antenna is mounted at the center of the positioner as the antenna under test (AUT) and adjusted to be at bore-sight level with the receive antenna. The reference calibration is repeated for each polarization of the receive antenna, with the reference antenna polarized parallel to the corresponding receive element. Figure 1 shows a typical range-calibration setup and calls out various components that are included in the measurement.

Typically, a signal generator or the output of a network analyzer is connected to the reference antenna by one or more cables, possibly through a power amplifier. The receive antenna is connected to a receiver or the input of a network analyzer through one or more additional cables, possibly through a preamplifier.

The power at the transmit antenna input port, P_t, is given in terms of the signal generator output, P_{SG}, by

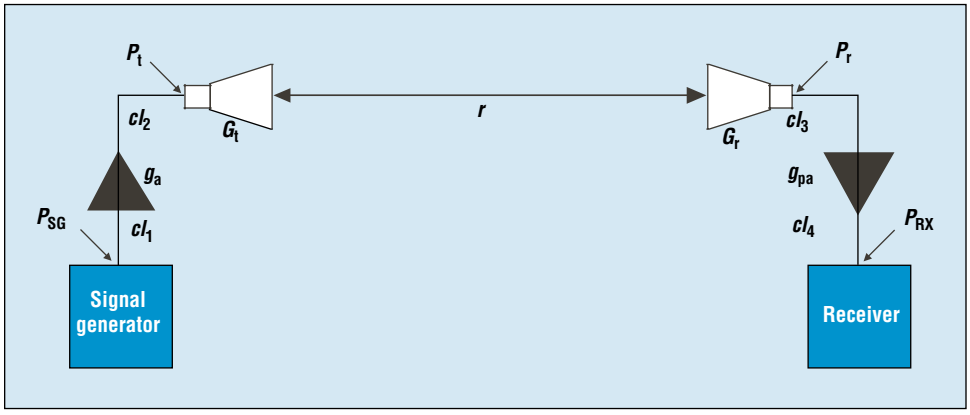

Figure 1. Some typical components of a range-calibration setup.

$$P_t = \frac{P_{SG} g_a}{cl_1 cl_2}, \quad (1)$$

where g_a is the gain of the amplifier, and cl_1 and cl_2 are the cable losses of the corresponding transmit cables.

The power at the receiver, P_{RX}, is given in terms of the power at the receive antenna output port, P_r, by

$$P_{RX} = \frac{P_r g_{pa}}{cl_3 cl_4}, \quad (2)$$

where g_{pa} is the gain of the preamplifier, and cl_3 and cl_4 are the cable losses of the corresponding receive cables.

If any of the components are missing, the corresponding gain or loss for that variable in the equation should be 1. In terms of decibels, these formulas become

$$P_t = P_{SG} + g_a - cl_1 - cl_2 \quad (3)$$

and

$$P_{RX} = P_r + g_{pa} - cl_3 - cl_4, \quad (4)$$

and the gain or loss of missing components would be 0 dB.

The Friis transmission equation governs the interaction between two antennas in the far field:

$$P_r = \frac{P_t G_t G_r \lambda^2}{(4\pi r)^2}, \quad (5)$$

where P_r is the power measured at the receive antenna output port; P_t is the power measured at the transmit antenna input port; G_t is the gain of the transmit antenna; G_r is the gain of the receive antenna; λ is the wavelength; and r is the separation between the two antennas (the range length).[1,2]

The exact definition of P_t is often a source of some confusion and is somewhat dependent on what terms are included in the definition of gain. If the antenna is perfectly matched to the source cable, then all power applied to the antenna is radiated (or absorbed by losses in the antenna). However, in the more common case of a mismatch between the source impedance and the antenna impedance, a portion of the energy is reflected back to the source so that the net power transmitted is the difference between the applied forward incident power and the power reflected back to the source:

$$P_{net} = P_{inc} - P_{refl}. \quad (6)$$

If a theoretical gain value is used in the Friis equation, then P_{net} should be used for P_t because the theoretical formula typically would not be able to account for the voltage standing wave ratio (VSWR) caused by the impedance mismatch. This requires either using a bidirectional coupler and power meter configuration at the transmit antenna to determine P_{net} directly, or measuring the VSWR of the antenna and performing additional calculations to predict the net power from the forward power.

If measured gain values are used, it is important to know how those gain values were determined and whether they already contain a contribution from the VSWR. Because any calibration technique is inherently governed by this same formula, the resulting gain will be different depending on whether VSWR effects have been accounted for separately. If not, the gain will be changed simply by the ratio of net power to forward power:

$$P_r = \frac{P_{net} G_{t\,net} G_r \lambda^2}{(4\pi r)^2} = \frac{P_{inc} (G_{t\,net} \cdot P_{net}/P_{inc}) G_r \lambda^2}{(4\pi r)^2} = \frac{P_{inc} G_{t\,inc} G_r \lambda^2}{(4\pi r)^2} \quad (7)$$

The difference between rms and peak field values can result in an immediate 3-dB error in reported measurement results.

An impedance mismatch is just as likely to happen with the receive antenna, leading to similar measurement issues, but it would not be as easy to observe directly because, in this case, the reflected energy would be reradiated. There is no good way to measure the forward and reflected received energy. However, the VSWR of the receive antenna can be used to determine this effect. Fortunately, the gain of the receive antenna does not need to be known exactly (other than to double-check the calibration result against theoretical predictions) because it will be measured as part of the range calibration process.

As indicated in Figure 1, other factors are typically involved in the measurement, unless power meters and directional couplers are used right at the antennas to measure the net transmitted and received power. These factors include cable losses and the gain of any power amplifiers or preamplifiers.

To minimize the uncertainty of resulting measurements, it is usually desirable to perform the range calibration with all cables in place and use the same configuration for both calibration and pattern measurements. Should any component be changed or damaged, the entire calibration must be redone. It is possible to perform individual calibrations on various system components, but each additional measurement increases the total measurement uncertainty involved. Therefore, it is preferable to calibrate the system as a whole whenever possible.

TRP

To determine exactly how to apply the range calibration, it is important to make a comparison between the desired measurement quantities and what will actually be measured by the test system. The primary quantity of interest is the TRP, which can be obtained by integrating the time-averaged power density of the radiated signal across the entire spherical surface enclosing the AUT.

The time-averaged power density of a radiating signal is given by the real part of the Poynting vector:

$$\rho = \frac{1}{2} Re(\vec{E} \times \vec{H}) = \frac{1}{2} \frac{|E|^2}{\eta} = \frac{|E_{\text{rms}}|^2}{\eta} = \frac{|E_{\text{rms}}|^2}{120\pi}, \tag{8}$$

where ρ is the time-averaged power density, E is the peak electric field strength, H is the peak magnetic field strength, E_{rms} is the root-mean-square (rms) electric field strength, and η is the impedance of free space (120π).[3, 4]

The factor of ½ in the definition of the power density originates from the time averaging of the power across a complete period. Although most reference materials and numerical analysis tools refer to wave magnitudes by their peak values,

$$\vec{E} = Ee^{-j\omega t}, \tag{9}$$

most measurement instrumentation reports rms values,

$$E_{\text{rms}} = \frac{1}{\sqrt{2}} E. \tag{10}$$

Therefore, when determining the power density from the rms electric field, the factor of ½ has already been accounted for. The difference between rms and peak field values can result in an immediate 3-dB error in reported measurement results if it is not treated correctly.

The TRP is given by integrating the power density across the surface of the reference sphere:

$$TRP = \int_{\theta=0}^{\pi} \int_{\phi=0}^{2\pi} \rho r^2 \sin(\theta) d\theta d\phi, \tag{11}$$

where TRP is the total radiated power, ρ is the time-averaged power density, r is the radius of the sphere (the range length), θ is the elevation angle, and ϕ is the azimuth angle.

The electric field generated at a point in the far field as a function of the transmitted power is given by

$$E = \frac{\sqrt{30 P_t G_t(\theta,\phi)}}{r}, \tag{12}$$

where E is the electric field generated at the distance r from the transmit antenna, P_t is the power measured at the transmit antenna input port, $G_t(\theta, \phi)$ is the angle-dependent gain of the transmit antenna, and r is the distance from the transmit antenna to the test point (the range length).[1]

Combining the equation for the power density with that of the electric field gives

$$\rho = \frac{P_t G_t(\theta,\phi)}{4\pi r^2}. \tag{13}$$

Combining this result with the equation for TRP gives

$$TRP = \frac{P_t}{4\pi} \int_{\theta=0}^{\pi} \int_{\phi=0}^{2\pi} G_t(\theta,\phi) \sin(\theta) d\theta d\phi. \tag{14}$$

Received Power

Unfortunately, the receiver used to perform the test cannot measure power density directly; instead, it measures received power (again, neglecting cable losses, etc.). A related quantity to the TRP would then be the total received power, given by integrating the received power across all of the measurement points of the AUT. The total power received is

$$TP_r = \int_{\theta=0}^{\pi} \int_{\phi=0}^{2\pi} P_r \sin(\theta) d\theta d\phi, \tag{15}$$

where TP_r is the total power received and P_r is the power measured at the receive antenna output port.

The received power is given by the Friis transmission equation described earlier, so in terms of the transmit power and the angle-dependent gain, the equation becomes

$$TP_r = \frac{P_t G_r \lambda^2}{(4\pi r)^2} \int_{\theta=0}^{\pi} \int_{\phi=0}^{2\pi} G_t(\theta,\phi) \sin(\theta) d\theta d\phi. \tag{16}$$

Because the desired value is TRP, the required correction factor is simply the ratio of TRP to the total power received:

$$\frac{TRP}{TP_r} = \frac{\frac{P_t}{4\pi} \int_{\theta=0}^{\pi} \int_{\phi=0}^{2\pi} G_t(\theta,\phi) \sin(\theta) d\theta d\phi}{\frac{P_t G_r \lambda^2}{(4\pi r)^2} \int_{\theta=0}^{\pi} \int_{\phi=0}^{2\pi} G_t(\theta,\phi) \sin(\theta) d\theta d\phi}, \tag{17}$$

which, when simplified, becomes

$$\frac{TRP}{TP_r} = \frac{4\pi r^2}{G_r \lambda^2}. \tag{18}$$

This constant makes sense because the factor is related to the range length and the gain of the receive antenna, both of which are exactly what needs to be calibrated out of the system. Going back to the Friis equation, the reference measurement performed with the reference antenna results in a site reference constant given by

$$C = \frac{P_r}{P_t} = \frac{G_t G_r \lambda^2}{(4\pi r)^2}, \tag{19}$$

where C is the ratio of received power to transmitted power. Substituting this into the previous equation gives a correction factor of

$$\frac{TRP}{TP_r} = \frac{G_t}{4\pi C}. \tag{20}$$

The required site-calibration constant is now represented in terms of the gain of the reference antenna and a single-path loss measurement for each polarization. The ratio C could contain contributions from other terms, such as cable loss and so forth, as long as those contributions are present in both the reference calibration and the pattern measurements.

Accounting for VSWR

The treatment of the transmit antenna VSWR is an important part of both the range calibration and the measurement of various antenna properties. In general, VSWR is a measurement of the mismatch between two transmission lines. It provides a measurement of the amount of signal being reflected back from the mismatch, which is directly related to the amount of energy that is transmitted.

For many antennas, the VSWR represents the largest component of the antenna efficiency (the rest results from ohmic losses in the antenna itself). To determine the contribution from VSWR, it is necessary to calculate the ratio of the net power to the forward power.

VSWR is defined as the ratio of maximum to minimum voltage on the transmission line and is given by

$$VSWR = \frac{V_{max}}{V_{min}} = \frac{V_{inc} + V_{refl}}{V_{inc} - V_{refl}}, \tag{21}$$

where V_{max} is the maximum voltage on the transmission line (feed cable), V_{min} is the minimum voltage on the transmission line, V_{inc} is the magnitude of the incident wave, and V_{refl} is the magnitude of the reflected wave.[5]

The reflection coefficient ρ (not to be confused with the power density described previously) is the ratio of reflected to incident waves and is given by

$$\rho = \frac{V_-}{V_+}, \tag{22}$$

or, in terms of impedance,

$$\rho = \frac{Z_L - Z_o}{Z_L + Z_o}, \tag{23}$$

where V_+ is the incident wave (magnitude and phase), V_- is the reflected wave (magnitude and phase), Z_o is the characteristic impedance of the transmission line (magnitude and phase), and Z_L is the impedance of the load line (magnitude and phase).

If the load impedance is equal to the characteristic impedance of the transmission line, the reflection coefficient would be zero because there is no mismatch in this case. In addition, unlike VSWR, the reflection coefficient has both magnitude and phase. The magnitude of the reflection coefficient is then

$$|\rho| = \frac{V_{refl}}{V_{inc}} = \frac{VSWR - 1}{VSWR + 1}. \tag{24}$$

The transmission coefficient τ is defined as the ratio of transmitted to incident waves and is given by

$$\tau = \frac{V_L}{V_+}, \tag{25}$$

or, in terms of impedance,

$$\tau = \frac{2Z_o}{Z_L + Z_o}, \tag{26}$$

where V_L is the wave transmitted through the mismatch to the load side (magnitude and phase).

By definition, $\tau - \rho = 1$. However, the transmission coefficient is not very useful for determining the net transmitted power from the VSWR because it also requires some knowledge of the impedance of the load. Although the necessary information could be determined from the reflection coefficient, it is considerably easier to determine the ratio of the reflected power to the incident power, and then use that to determine the net transmitted power:

$$\frac{P_{refl}}{P_{inc}} = \frac{V_{refl}^2}{V_{inc}^2} = |\rho|^2, \tag{27}$$

so that

$$\begin{aligned} P_{net} &= P_{inc} - P_{refl} \\ &= P_{inc} - P_{inc} \cdot |\rho|^2 \\ &= P_{inc}\,(1 - |\rho|^2). \end{aligned} \tag{28}$$

This results in a VSWR correction factor given in dB by

$$\begin{aligned} C_{VSWR} &= 10\log_{10}(1 - |\rho|^2) \\ &= 10\log_{10}\left(\frac{4 \cdot VSWR}{(VSWR + 1)^2}\right). \end{aligned} \tag{29}$$

The VSWR component covered here is not the only antenna VSWR term related to antenna measurements. If an antenna is not in a free-space environment, energy reflected back from other objects will affect the VSWR measurement. However, this term is a measure of the antenna's interaction with its environment rather than a measurement of an inherent property of the antenna.

Care should be taken when measuring VSWR to be used for range calibrations to ensure that the measurement represents a true free-space VSWR. A simple way to do this is to alter the orientation and location of the reference antenna when measuring VSWR. If no variation is seen in the resulting VSWR measurements, then the environment probably does

not have a significant effect.

Gain, Directivity, Efficiency, and EIRP

Once the range has been calibrated, a number of antenna properties can be determined from the pattern measurement. The first property of interest is EIRP. EIRP is the power required for a theoretical isotropic radiator (one that radiates the same power in all directions) to generate the same field level in all directions as the maximum field seen from the AUT. Starting from the definition of TRP, EIRP is given by

$$EIRP = \int_{\theta=0}^{\pi} \int_{\phi=0}^{2\pi} \rho_{max} r^2 \sin(\theta) d\theta d\phi, \tag{30}$$

where ρ_{max} is the maximum time-averaged power density found over the surface of the measurement sphere.

Assuming that the maximum power density can be defined using the bore-sight gain of the AUT,

$$\rho_{max} = \frac{P_t G_t}{4\pi r^2}. \tag{31}$$

Combine this with the equation for EIRP to get

$$\begin{aligned} EIRP &= \int_{\theta=0}^{\pi} \int_{\phi=0}^{2\pi} \frac{P_t G_t}{4\pi r^2} r^2 \sin(\theta) d\theta d\phi, \\ &= P_t G_t . \end{aligned} \tag{32}$$

EIRP is simply the transmitted power increased by the AUT gain, which brings some clarity to the definition of gain. Gain (over isotropic) is defined as the increase in received signal from the AUT over that which would be received from an isotropic radiator with the same source power. Therefore, to create an isotropic radiator that generates the same field level as the maximum seen from the AUT, the source power must be increased by the gain.

Rearranging the equation for EIRP gives the definition of gain:

$$G_t = \frac{EIRP}{P_t}, \tag{33}$$

where P_t is often referred to as the *antenna-port input power* (APIP). Again, there is the question of whether this term should refer to the incident power or whether it should refer to the net power. This decision affects the calculation of the efficiency of the antenna.

The ratio of EIRP to TRP is defined as the *directivity* of the antenna:

$$\begin{aligned} D = \frac{EIRP}{TRP} &= \frac{P_t G_t}{\frac{P_t}{4\pi} \int_{\theta=0}^{\pi} \int_{\phi=0}^{2\pi} G_t(\theta,\phi) \sin(\theta) d\theta d\phi} \\ &= \frac{4\pi}{\int_{\theta=0}^{\pi} \int_{\phi=0}^{2\pi} \Delta_t(\theta,\phi) \sin(\theta) d\theta d\phi}, \end{aligned} \tag{34}$$

where $\Delta_t(\theta, \phi)$ is the relative magnitude of the AUT pattern at any angle with respect to the maximum.[2] For an isotropic radiator, $\Delta_t(\theta, \phi) = 1$, so that $D = 1$. For any real antenna, $\Delta_t(\theta, \phi) < 1$ for much of the surface, resulting in $D > 1$. Directivity is the only term related to the antenna gain, which is solely a relative term. Range calibration does not show up in this equation.

As with the TRP measurement, the measurement system is only capable of measuring received power, so instead of EIRP, the corresponding value calculated would be the effective isotropic received power:

$$\begin{aligned} EIP_r &= \int_{\theta=0}^{\pi} \int_{\phi=0}^{2\pi} P_{r\,max} \sin(\theta) d\theta d\phi \\ &= 4\pi P_{r\,max}, \end{aligned} \tag{35}$$

where $P_{r\,max}$ is the maximum received power from the pattern measurement.

Assuming again that the maximum received power is the bore-sight transmission response, the same site-reference constant, C, can be used:

$$\frac{EIRP}{EIP_r} = \frac{P_t G_t}{4\pi P_{r\,max}} = \frac{G_t}{4\pi C}. \tag{36}$$

It is apparent that the same range calibration holds in this case as well. Therefore, the directivity can also be represented directly in terms of measured quantities as

$$D = \frac{EIP_r}{TP_r}. \tag{37}$$

The efficiency of the AUT is defined as the ratio of TRP to APIP. The choice of defining APIP as incident power or net power determines whether VSWR is part of the efficiency term. If the net power definition is used, the efficiency only represents the ohmic losses of the antenna and not the mismatch effects:

$$\varepsilon = \frac{TRP}{P_t}. \tag{38}$$

Comparing this to the definition of gain and directivity makes it clear that gain is given by the product of directivity and efficiency:

$$G_t = \frac{EIRP}{P_t} = \frac{EIRP}{TRP} \frac{TRP}{P_t} = D\varepsilon. \tag{39}$$

If the AUT has no losses or mismatch, the directivity and gain should be equivalent.

Other Antenna Properties

There are plenty of other properties that can be determined from an antenna pattern, such as front-to-back ratio, average radiated power, average gain, and beam widths. The calculation of most of these properties is straightforward, usually using simple formulas. The most important part of many of the calculations is the data search algorithms used to find values like the maximum point, minimum point, and –3-dB points.

Some of these antenna properties have little or no meaning for some antennas. In addition, the orientation of the AUT can affect the result of an automated calculation without additional input from the user to indicate the desired alignment information. For example, the meaning of E- and H-plane beam widths is commonly understood. However, if an AUT is randomly oriented for the pattern test, or has an unusual pattern, there is no simple way to determine automatically what constitutes each plane.

CTIA Requirements

The Cellular Telecommunications and Internet Association (CTIA) has developed some very specific antenna-property requirements in addition to the EIRP and TRP measurements.[4] One of these is the near-horizon partial radiated power, which is used to determine the power radiated in a small band (typically ±22.5° or ±45°) along the azimuth axis. This requirement is intended to determine how a cellular phone will interact with the network of cellular base stations arranged around it along the horizon during normal operation. The orientation of the AUT will have a great effect on this result, so the standard calls out precise positioning requirements for the phone.

Because a cellular phone has both transmit and receive modes, the CTIA standard also contains receive property requirements, including total isotropic sensitivity (TIS) and near-horizon partial isotropic sensitivity (NHPIS), in addition to the radiated pattern requirements. These values are calculated from the received power pattern instead of the transmitted power pattern. Because the CTIA standard is still in draft form and subject to change, the details of these calculations are not covered in this article.

Conclusion

The techniques for complex pattern measurement are rather straightforward, but the calculations involved in determining certain antenna properties can be much more complicated. Nonetheless, with appropriate care and understanding of the associated quantities, it is not difficult to obtain excellent results.

The information provided in this article can help even the novice RF or EMC engineer to determine a variety of antenna properties.

References

1. "Antenna Calculations," *ETS-Lindgren Antenna Catalog* (Cedar Park, TX: ETS-Lindgren, 2002), 71.
2. CA Balanis, *Antenna Theory, Analysis and Design* (New York: Harper & Row, 1982), 29, 65.
3. JD Jackson, *Classical Electrodynamics*, 2nd ed. (New York: Wiley, 1975), 347.
4. "Method of Measurement for Radiated RF Power and Receiver Performance, Draft Revision 1.2" (Washington, DC: Cellular Telecommunications and Internet Association, 2001).
5. BC Wadell, *Transmission Line Design Handbook* (Boston: Artech House, 1991), 497.

Michael D. Foegelle, PhD, is senior principal design engineer at ETS-Lindgren (Cedar Park, TX). He can be reached at 512-531-6444 or michael.foegelle@emctest.com. ■